CrystEngComm

Accepted Manuscript

ROYAL SOCIETY OF CHEMISTRY

www.rsc.org/crystengcomm

CrystEngComm

ARTICLE

A Porous Lanthanide Metal-Organic Framework Based on a Flexible Cyclotriphosphazene-Functionalized Hexacarboxylate Exhibiting Selective Gas Adsorption

Received 00th January 20xx,
Accepted 00th January 20xx

DOI: 10.1039/x0xx00000x

www.rsc.org/

Yajing Ling,[a] Jingjing Jiao,[a] Mingxing Zhang,[b] Huiming Liu,[a] Dongjie Bai,[a] Yunlong Feng,[a] and Yabing He,[a*]

Design and synthesis of robust porous lanthanide-based metal-organic frameworks (Ln-MOFs) from flexible organic ligands is currently a formidable task to chemists. In this work, a porous Ln-MOF based on a flexible cyclotriphosphazene-functionalized organic ligand, hexakis(4-carboxylatephenoxy) cyclotriphosphazene, has been solvothermally synthesized. Single-crystal X-ray diffraction analyses show that the compound exhibits a three-dimensional structure built up from rod-shaped secondary building units which link to each other through the organic ligands to form open frameworks with rectangular channels along the crystallographic *a* direction. Remarkably, although the flexible ligand was used, the Ln-MOF material after desolvation exhibited permanent porosity which has been established by various gas adsorption isotherms, displaying selective adsorption of C_2 hydrocarbons over CH_4 at room temperature. This work presents a rare example of permanently porous Ln-MOFs based on flexible ligands exhibiting selective gas adsorption behaviours.

1. Introduction

Metal-organic frameworks (MOFs), also called porous coordination polymers (PCPs), are a burgeoning subclass of crystalline porous functional materials consisting of metal ions or metal-containing clusters connected by multi-dentate organic linkers to form multidimensional networks. Compared to conventional porous materials such as zeolite and activated carbon, MOFs have given to the chemists the opportunity of tuning the pore sizes by rational selection of the organic ligands and metal ions, and grafting various functionalities by pre-synthetical or post-synthetical modification. These special structural characters make MOFs a potential platform for a wide range of applications in various fields such as gas storage and separation,[1] heterogeneous catalysis,[2] chemical sensing[3] and drug delivery.[4]

In terms of MOFs for gas adsorption, lanthanide-based MOFs (Ln-MOFs), a subfamily of MOFs, have gained less attention compared to the transition metal MOF counterparts. This is mainly because it remains a great challenge to synthesize robust porous Ln-MOFs. The large coordination number (typically from 6 to 10) and flexible coordination geometry of lanthanide ions frequently result in the formation of either densely packed structures or only structurally porous frameworks which are readily collapsed once the terminal and free solvent molecules are removed during the activation. Considering these limitations, current research on Ln-MOFs mainly focused on their magnetic and photoluminescence properties originating from 4f electrons of lanthanide ions,[5] while seldom on their gas adsorption behaviour.[6] As far as we know, only very few Ln-MOFs showed permanent porosities and significant gas uptakes.[7] In addition to the great difficulty in building robust porous Ln-MOFs, equally challenging is construction of robust porous MOFs from flexible organic ligands because compared to rigid organic ligands, the conformational freedom and flexibility of flexible organic ligands make the frameworks very difficult to stabilize. Therefore, the design and synthesis of robust Ln-MOFs from flexible organic ligands is currently a formidable task to chemists. To the best of our knowledge, relatively few such Ln-MOFs have been realized so far. Exploring such Ln-MOFs will be of highly fundamental interest.

In continuation of our recent research interest in constructing robust porous MOFs from a flexible organic ligand for selective gas separation,[8] we chose a cyclotriphosphazene functionalized hexacarboxylic acid, hexakis(4-carboxylatephenoxy)cyclotriphosphazene (H_6L, Scheme 1), as a flexible organic ligand in this work to build Ln-MOFs, which is based on the following considerations. 1) cyclotriphosphazene and its derivatives have found widespread use as building blocks in supramolecular and materials chemistry,[9] while their MOF chemistry remained less developed;[8, 10] 2) The versatile

[a] College of Chemistry and Life Sciences, Zhejiang Normal University, Jinhua 321004 China. E-mail: heyabing@zjnu.cn.
[b] State Key Laboratory of Coordination Chemistry, School of Chemistry and Chemical Engineering, Nanjing University, Nanjing 210093, China.

Electronic Supplementary Information (ESI) available: PXRD (Fig. S1), TGA (Fig. S2), N_2 isotherms at 77 K of **ZJNU-61(Ho)** activated at different temperatures (Fig. S3), BET plot (Fig. S4), Van't Hoff isochores for C_2H_2, C_2H_4, C_2H_6 and CH_4 adsorption (Fig. S5), FTIR (Fig. S6), BET surface area in the reported Ln-MOFs (Table S1), Crystal data and structure refinement parameters (Table S2), CCDC No 1471569. See DOI: 10.1039/x0xx00000x

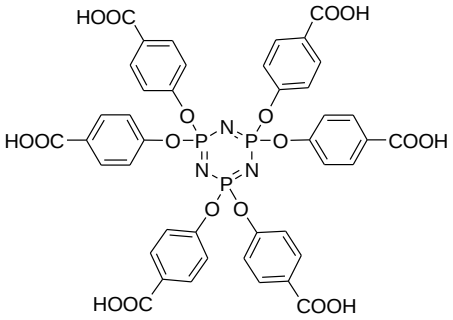

Scheme 1 The organic linker H_6L used to construct **ZJNU-61**(Ho).

coordination modes of carboxylate groups on this ligand, and the conformational freedom of the ligand due to the presence of a –o– spacer between the peripheral benzoate and the central cyclotriphosphazene units, coupled with the highly flexible coordination geometries of the lanthanide ions, may work in synergy to afford opportunities in discovering unusual framework structures; 3) According to HSAB (hard and soft acid and base) principle, lanthanide ions prefer binding carboxylate oxygen atoms rather than nitrogen atoms, so the N atoms of central cyclotriphosphazene can act as functional sites to direct selective molecular recognition. In this contribution, we wish to report the successful preparation of a Ln-MOF constructed from this flexible organic ligand, whose permanent porosity has been unambiguously established as shown in diverse gas adsorption isotherms. The Ln-MOF material exhibited selective adsorption of C_2 hydrocarbons over CH_4 at ambient temperature, making it a potential adsorbent for the natural gas purification. It is a rare example of permanently porous Ln-MOFs based on a flexible ligand for selective gas adsorption.

2. Experimental

2.1 Materials and general methods

All the chemicals were commercially available and used as received without further purification unless otherwise noted. $Ho(NO_3)_3{\cdot}6H_2O$ (purity: 99.99%) was purchased from Jinan Henghua Sci. & Tec. Co. Ltd. The organic linker was synthesized according to the reported methods.[8] Fourier Transform infrared (FTIR) spectra were recorded in the range of 400-4000 cm^{-1} on a Nicolet 5DX FT-IR spectrometer using KBr pellets. Elemental analyses (C, H, and N) were measured with a Perkin–Elmer 240 CHN analyser. Thermogravimetric analyses (TGA) were performed on a Netzsch STA 449C thermal analyser with a heating rate of 5 K min^{-1} under a nitrogen atmosphere. Powder X-ray diffraction (PXRD) measurements were recorded on a Philips PW3040/60 automated powder diffractometer using Cu-K_a radiation (λ = 1.54056 Å) between 2ϑ values of 5 and 40°. The simulated powder pattern was obtained using the program Mercury 2.0 based on the single-crystal CIF file. Gas sorption isotherm measurements were performed on a Micrometrics ASAP 2020 HD88 surface-area-and-pore-size analyser. The gases used have the following specifications (volume percentage): N_2 99.9999%, CH_4 99.99%, C_2H_2 99.5%, C_2H_4 99.5%, and C_2H_6 99.5%. The sorption measurement was maintained at 77 K with liquid nitrogen and at other specified temperatures by using a circulating water bath (Julabo F12).

2.2 X-ray crystallographic data collection and refinement

X-ray diffraction data were collected using a Bruker SMART APEX II with graphite monochromated Mo K_α radiation (λ = 0.71073 Å) at a low temperature of 193(2) K. The structure was solved by the direct method and refined by the full-matrix least-squares on F^2 using the SHELXTL-2014 program. The unit cell includes a large region of disordered solvent molecules, which cannot be located in the electron density map, and thereby were squeezed out with the help of PLATON/SQUEEZE;[11] the structure was then refined again using the data generated. The hydrogen atoms were treated by geometrical positions. It should be mentioned that in this heavy-atom structure it was not possible to see clear electron-density peaks in difference maps which would correspond with acceptable locations for the H atoms bonded to a water oxygen atom and for the H atoms bonded to methyl carbon C86, the refinement was completed with no allowance for these H atoms in the model. Crystallographic data and other pertinent information for the compound are summarized in Table S2 in the supporting information. Complete crystallographic data (CCDC NO. 1471569) for the compounds reported in this paper have been deposited in the Cambridge Crystallographic Data Centre.

2.3 Synthesis of ZJNU-61(Ho)

A mixture of $Ho(NO_3)_3{\cdot}6H_2O$ (5.0 mg, 11.21 μmol), the organic ligand (5.0 mg, 5.22 μmol) and thiophene 2,5-dicarboxylic acid (1.0 mg, 5.81 μmol) was added to a mixed solvent of *N*,*N*-dimethyl acetamide (DMA, 1.0 mL) and H_2O (0.5 mL) in a 20 mL Teflon-lined stainless steel autoclave. After the addition of 45 μL of 6 M HCl, the autoclave was sealed, heated to 393 K in 4 h, and held at this temperature for 3 days. After the autoclave was slowly cooled to 308 K within 3 days, colourless strip-shaped crystals were collected by filtration, and washed with DMA. The yield is 54% based on the organic ligand. Based on the single-crystal structural analysis, TGA, and elemental analysis, **ZJNU-61(Ho)** can be best formulated as $[Ho_4L_2(CH_3COO)(H_2O)]{\cdot}(CH_3)_2NH_2{\cdot}20DMA$. Elemental analysis for $C_{168}H_{241}N_{27}O_{59}P_6Ho_4$, calcd (%): C, 45.56; H, 5.49; N, 8.54. Found (%): C, 45.41; H, 5.48; N, 8.64; Selected FTIR (KBr, cm^{-1}): 3419, 1603, 1549, 1421, 1267, 1201, 1180, 1159, 1097, 1016, 951, 889, 866, 789, 764, 741, 698, 638, 623, 557.

2.4 Calculation of isosteric heats of adsorption

The isosteric heats of gas adsorption, Q_{st}, for a given amount adsorbed were calculated using the Clausius-Clapeyron equation assuming that Q_{st} does not vary with the temperature, expressed as

$$Q_{st} = -R\left(\frac{\partial \ln P}{\partial (1/T)}\right)_q \quad (1)$$

where *P, T, R*, and *q* stand for the pressure, the temperature, the gas constant, and the adsorption amount. Specifically, a

linear fitting of ln*P* versus 1/*T* for each loading was provided in Fig. S5 in the supporting information. The slope of the line is $-Q_{st}/R$, and thus Q_{st} can be derived from the slope of the line: $Q_{st} = -R \times$ slope.

3 Results and discussion

3.1 Synthesis and characterization

Solvothermal reaction of the flexible organic linker H_6L with Ho(III) nitrate hexahydrate under carefully selected conditions yielded colourless crystals of a Ln-MOF which we termed **ZJNU-61**(Ho). It is important to note the importance of thiophene-2,5-dicarboxylate for the synthesis of the Ln-MOF material. The omission of thiophene-2,5-dicarboxylate from the synthesis leads to the formation of materials unsuitable for single-crystal X-ray diffraction experiments. The structure was characterized by single-crystal X-ray diffraction and the phase purity was confirmed by a good agreement between the measured X-ray diffraction pattern and the calculated one (Fig. S1). TGA under a nitrogen atmosphere shows an initial weight loss of *ca.* 38% up to 623 K, corresponding to the loss of free guest molecules trapped in the channels (calcd: 39.7%), followed by a plateau region until 733 K, where the solid starts to decompose rapidly (Fig. S2).

3.2 Description of crystal structure

Single-crystal X-ray analysis reveals that **ZJNU-61**(Ho) crystallizes in the monoclinic system, the chiral space group of $P2_1$, which is atypical considering that the ligand is an achiral building block. Besides the guest molecules, the asymmetric unit of **ZJNU-61**(Ho) consists of four crystallographically independent Ho^{3+} ions, two fully deprotonated ligands, one acetate ion, and one aqua molecule (Fig. 1). Regarding the organic linker, three of the six carboxylatephenoxy arms around the central cyclotriphosphazene ring of the ligand are situated above the central scaffold, and the other three below (Fig. 2b, 2c). The average P–N distance is 1.5837 Å, and the average N–P–N and P–N–P angles are 117.85° and 120.98°, respectively, which are very similar to the ones previously reported for cyclotriphosphazene derivatives.[8, 10] The cyclotriphosphazene ring nitrogen atoms do not participate in coordination with Ho^{3+} ions, whilst all six carboxylate groups of the organic linker are deprotonated and involved in metal

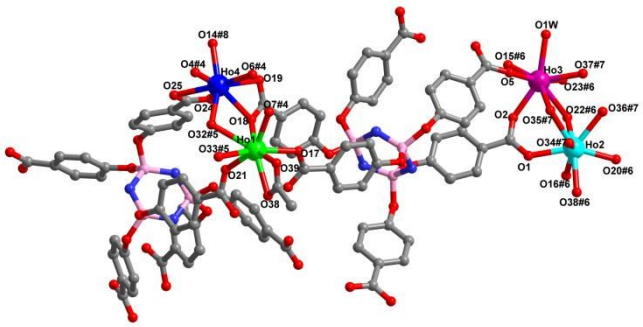

Fig. 1 The perspective view of the asymmetric unit with partial atoms labelled. Symmetry codes: #4 -*x*+1, *y*+1/2, -*z*+1; #5 -*x*+1, *y*+1/2, -*z*; #6 -*x*, *y*-1/2, -*z*+1; #7 *x*, *y*, *z*+1; #8 *x*+1, *y*, *z*.

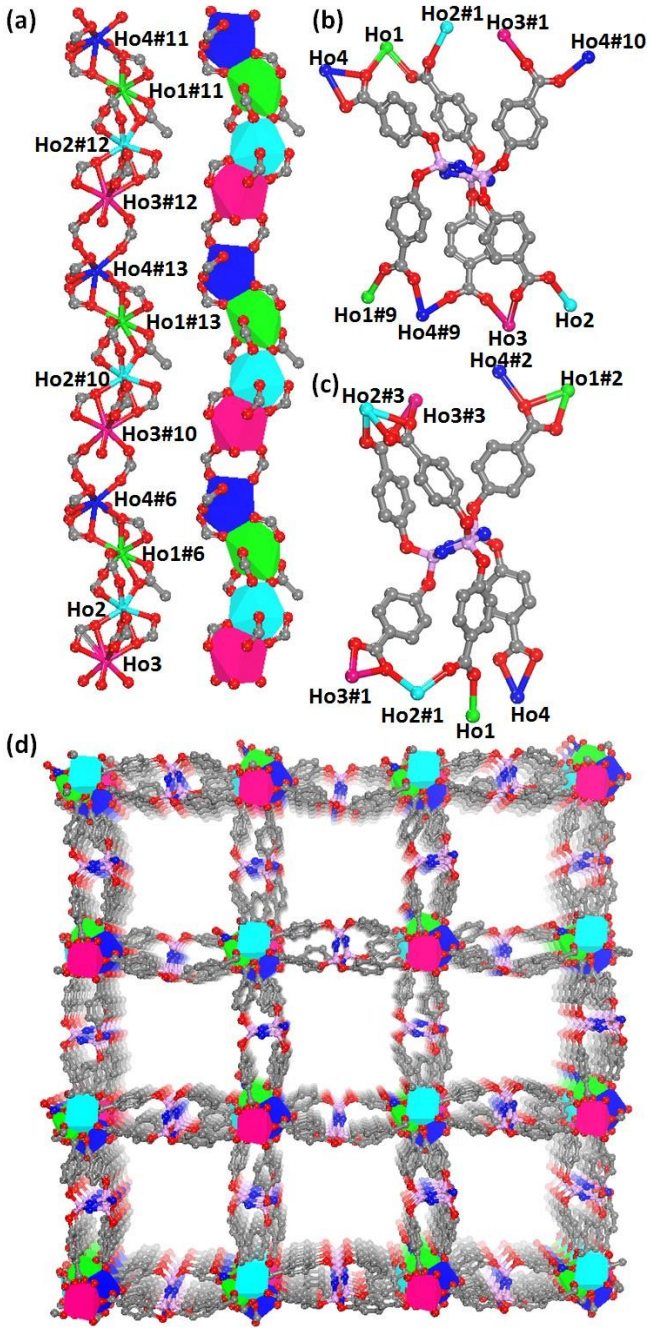

Fig. 2 View of the single-crystal X-ray diffraction structure of **ZJNU-61**(Ho) showing (a) the inorganic "Ho-carboxylate" chain, represented by ball-and-stick and polyhedral model, respectively; (b) two different types of coordination modes exhibited by the organic ligands; and (d) one-dimensional square channels along the crystallographic *a* axis. Symmetry codes: #1 -*x*, *y*+1/2, -*z*+1; #2 -*x*+1, *y*-1/2, -*z*; #3 *x*, *y*, *z*-1; #6 -*x*, *y*-1/2, -*z*+1; #9 -*x*+1, *y*-1/2, -*z*+1; #10 *x*-1, *y*, *z*; #11 -2-*x*, -0.5+*y*, 1-*z*; #12 -2+*x*, *y*, *z*; #13 -1-*x*, -0.5+*y*, 1-*z*.

coordination. It is noteworthy that the ligand displays two different types of coordination modes with the Ho^{3+} centres, shown in the Fig. 2b and 2c. In the first mode (Fig. 2b), the ligand has a μ_9-connectivity and binds to nine Ho^{3+} centres through six carboxylate groups adopting two different coordination modes that can be described as bridging mode (μ_2:$\eta^1\eta^1$) and bridging-chelating mode (μ_2:$\eta^1\eta^2$), respectively.

In the second mode (Fig. 2c), the ligand acts as a μ_8-bridging mode to connect eight Ho^{3+} centres through six carboxylate groups adopting three different coordination modes that can be described as bridging mode (μ_2:$\eta^1\eta^1$), bridging-chelating mode (μ_2:$\eta^1\eta^2$), and chelating mode (μ_1:$\eta^1\eta^1$), respectively. All the four crystallographically unique Ho(III) atoms are eight coordinated, forming a [HoO_8] unit which can be best represented as distorted trigonal dodecahedron geometry. Concretely, The Ho1 atom is eight-coordinated by six carboxylate oxygen atoms (O7#4, O17, O18, O21, O32#5, O33#5) from four different ligands and two oxygen atoms (O38, O39) belonging to acetate ions. The coordination environment of Ho2 atom is defined by seven carboxylate oxygen atoms (O1, O16#6, O20#6, O22#6, O34#7, O35#7, O36#7) stemming from four different ligands and one oxygen atom (O38#6) coming from acetate ion. The eight oxygen atoms surrounding Ho3 atom is provided by seven carboxylate oxygen atoms (O2, O5, O15#6, O22#6, O23#6, O35#7, O37#7) from four different ligands and one oxygen atom (O1w) belonging to the terminal water molecule. Ho4 is exclusively coordinated by eight carboxylate oxygen atoms (O4#4, O6#4, O14#8, O18, O19, O24, O25, O32#5) from five different ligands. The Ho-$O_{carboxylate}$ bond distance is in the range of 2.2394(10)-2.6000(8) Å, comparable to the reported values in other Ho-carboxylate complexes.[12] Each {$Ho2O_8$} polyhedron connects with one neighboring {$Ho3O_8$} polyhedron *via* edge sharing, and one neighboring {$Ho1O_8$} polyhedron *via* corner sharing. Each {$Ho1O_8$} polyhedron connects with one neighboring {$Ho2O_8$} polyhedron *via* corner sharing and one neighboring {$Ho4O_8$} polyhedron *via* edge sharing. In this way, these connectivities link the polyhedra into a tetranuclear Ho4 cluster, which is further bridged by carboxylate groups to form a 1D chiral "Ho-carboxylate" inorganic chain serving as 1D infinite rod-shaped secondary building unit parallel to the crystallographic *a* axis (Fig. 2a). The average separation between adjacent Ho^{3+} ions is 4.2965 Å. Notably, a close inspection of the structure discloses that the 1D chain is left-handed helical with the helical pitch of 15.8769(5) Å, which is particularly rare in Ln-MOFs. Furthermore, these chains are cross-linked together through

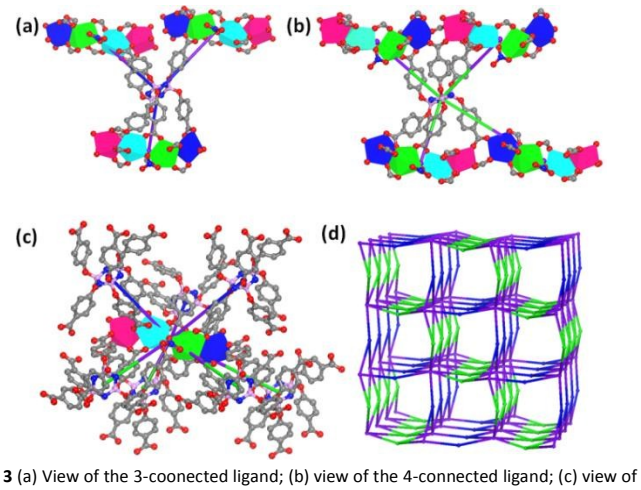

Fig. 3 (a) View of the 3-coonected ligand; (b) view of the 4-connected ligand; (c) view of 7-connected 7 cluster; (d) schematic representation of (3,4,7)-connected net with the point symbol of {$4\cdot6^2$}{$4^4\cdot6^2$}{$4^8\cdot6^{13}$}.

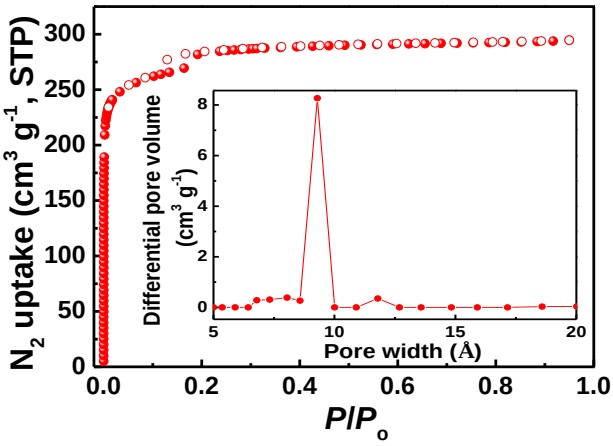

Fig. 4 N_2 adsorption-desorption isotherm of **ZJNU-61a**(Ho) at 77 K. Solid and open symbols represent adsorption and desorption, respectively. The inset shows the pore size distribution for **ZJNU-61a**(Ho) calculated by DFT.

organic ligands to form a non-interpenetrated 3D anionic network structure. There exist one-dimensional square channels of about 10 Å along the crystallographic *a* axis (Fig. 2d), taking into account the van der Waals radius of the atoms, which are occupied by the solvent molecules and dimethylammonium counterions, which are formed *in situ* upon heating of DMA through the well-established decomposition reaction. The PLATON analysis revealed that the solvent accessible space for the desolvated phase is 4775.8 $Å^3$ *per* unit cell or 56.3% of the total volume.

Topologically, two different types of the organic ligands were linked by three and four {Ho4} clusters and can be considered as 3-connected and 4-connected nodes, respectively (Fig. 3a,b), while the {Ho4} cluster is linked by seven neighbouring L^{6-} ligands and can be taken as 7-connected node (Fig. 3c); thus, the overall structure can be simplified as 3,4,7-c 3-nodal MoP_2-type net with Point (Schläfli) symbol of {$4\cdot6^2$}{$4^4\cdot6^2$}{$4^8\cdot6^{13}$} analysed by TOPOS software (Fig. 3d).

3.3 Permanent Porosity

The porosity of the Ln-MOF material was investigated by nitrogen sorption analysis at 77 K. Prior to measurement, the as-synthesized sample was solvent-exchanged with dry low-boiling-point acetone followed by evacuation under dynamic vacuum at 333 K until the degassed rate reached 3 μmHg min^{-1}, forming the desolvated framework **ZJNU-61a**(Ho) (thereafter, "a" represents the activated form of MOF materials). The reason why a temperature of 333 K is employed as activation temperature is that the maximum amount of nitrogen adsorbed at 77 K remains almost the same when the activation temperature is further increased (Fig. S3). As shown in Fig. 4, the isotherm shows two distinct adsorption steps with small hysteresis over the relative pressure range of 0.08-0.2, indicating a certain degree of flexibility in the material. Fitting the Brunauer–Emmett–Teller (BET) equation to the N_2 adsorption isotherm gives an estimated surface area of 1059 m^2 g^{-1} (Fig. S4). The BET surface area for **ZJNU-61a** (Ho) lies

towards the upper end compared to other Ln-MOFs (Table S1). The total pore volume estimated from the amount of N_2 adsorbed at maximum relative pressure is 0.456 cm^3 g^{-1}. The mean pore size obtained from the DFT model is predominantly around 0.93 nm (the inset in Fig. 4), which is close to the size of the 1D channel determined from the crystal structure.

3.4 Selective gas separation

Natural gas is one of the most important energy resources worldwide and its purification is one of the important objectives in the petrochemical industry. Natural gas is primarily composed of methane, and also contains light hydrocarbons such as ethane, ethylene, and acetylene. Light hydrocarbons present in natural gas have significantly enhanced value as petrochemical feedstocks rather than as components of natural gas used as fuels. For example, ethane is a key feedstock in industrial ethylene production. For the purpose of effective utilization of energy, the separation and purification of natural gas is therefore very essential and important. The conventional cryogenic distillation for such a separation is very energy-consuming due to the similar boiling points of the components. Recent reports have demonstrated the advantage of MOFs for natural gas purification and separation.[13]

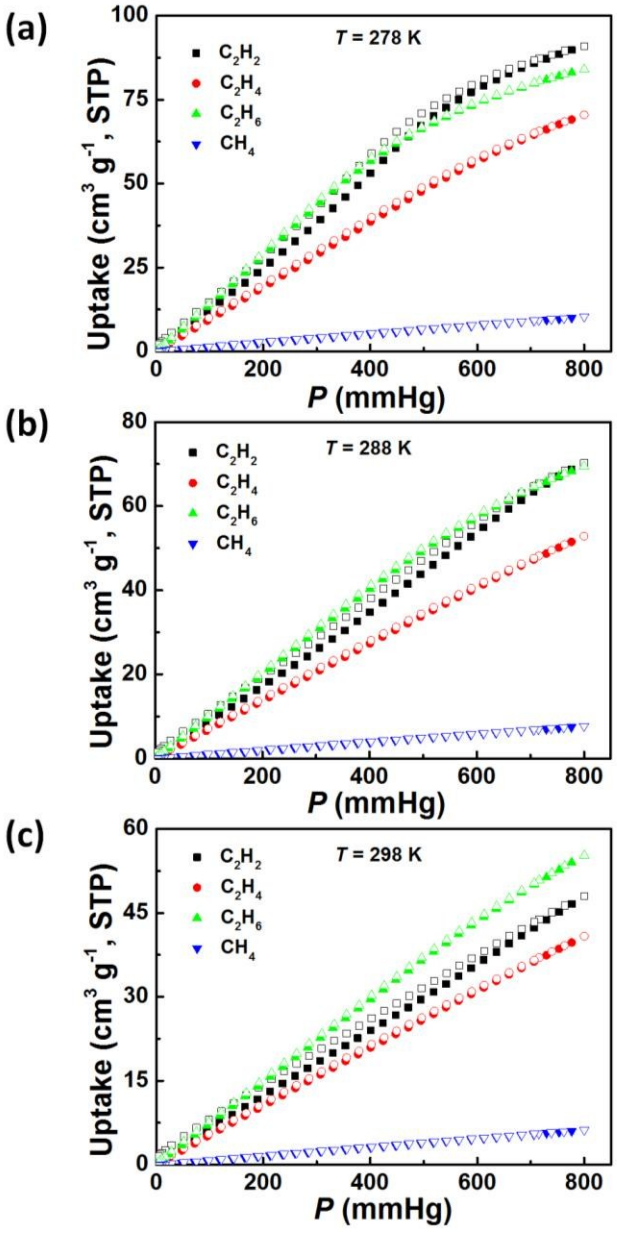

Fig. 5 C_2H_2, C_2H_4, C_2H_6 and CH_4 adsorption isotherms of **ZJNU-61a**(Ho) at 278 K (a), 288 K (b) and 298 K (c), respectively. Solid and open symbols represent adsorption and desorption, respectively. STP = standard temperature and pressure.

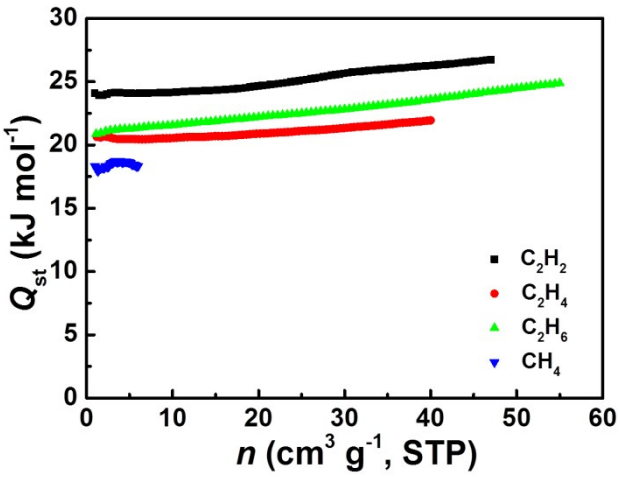

Fig. 6 The isosteric heat of adsorption for C_2H_2, C_2H_4, C_2H_6 and CH_4.

Establishment of permanent porosity prompts us to examine its utility as an adsorbent for purifying natural gas. Accordingly, we carried out C_2H_2, C_2H_4, C_2H_6 and CH_4 adsorption experiments at 278 K, 288 K and 298 K, respectively. As shown in Fig. 5, all gas sorptions were almost reversible and no significant hysteresis was observed. At 298 K and 1 atm, the adsorption amounts of C_2H_2, C_2H_4, C_2H_6 and CH_4 are 48.0, 40.8, 55.3, and 6.2 cm^3 (STP) g^{-1}, respectively, which increase to 91.0, 70.5, 84.0 and 10.3 cm^3 (STP) g^{-1} when the temperature is decreased to 278 K. The gas adsorption amounts are moderate, which may be due to the existence of large and straight channels without any polyhedral cages in the structure. It is noteworthy that C_2 hydrocarbon adsorptions of Ln-MOFs have been rarely studied to date.[7k] The gravimetric uptakes of C_2 hydrocarbons are comparable to those reported in a cationic MOF ZJU-48a under similar conditions.[14] The large discrepancy on adsorption capacities between C_2 hydrocarbons and CH_4 indicates that **ZJNU-61a**(Ho) is a promising material for selective separation of C_2 hydrocarbons from methane. To evaluate its separation selectivity for light hydrocarbons, we calculated the adsorptive selectivity of C_2 hydrocarbons over CH_4 using Henry's Law. The Henry's law selectivities for C_2H_2, C_2H_4, C_2H_6 over CH_4 in **ZJNU-61a**(Ho) are 9.9, 7.8, and 11.1 at 298 K and 10.5, 7.7, and 10.9 at 278 K, respectively, which are moderate compared to those reported for MOFs with high density of open metal sites such as MOF-74.[15]

The isosteric heat (Q_{st}) of gas adsorption revealing the affinity between the framework and gas molecule was calculated from the gas isotherms collected at 278 K, 288 K

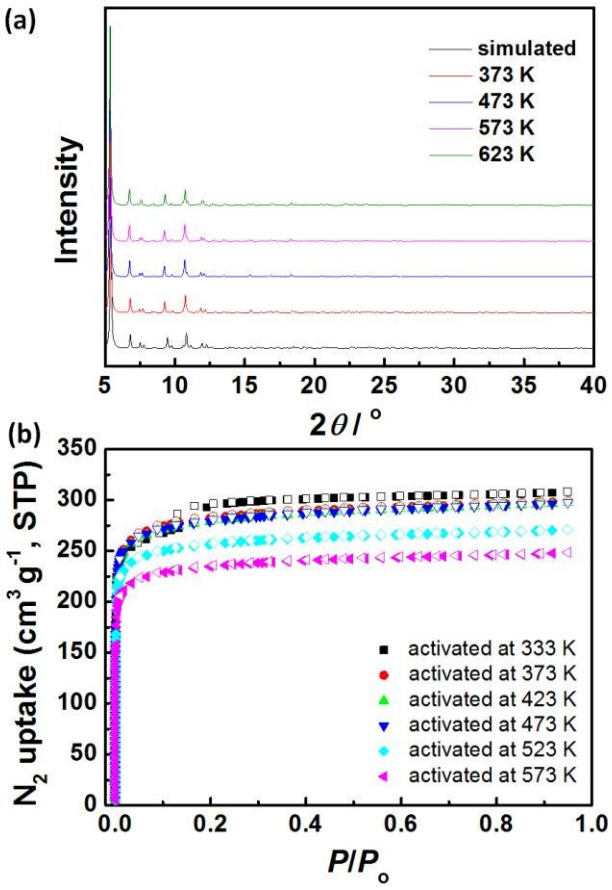

Fig. 7 (a) Variable-temperature PXRD patterns of **ZJNU-61**(Ho) observed in the temperature range up to 623 K; (b) N_2 adsorption-desorption isotherms at 77 K of **ZJNU-61**(Ho) activated at different temperatures. Solid and open symbols represent adsorption and desorption, respectively.

and 298 K employing the Clausius-Clapeyron equation. As shown in Fig. 6, the adsorption enthalpies of C_2H_2, C_2H_4, C_2H_6 and CH_4 at low coverage (2.0 cm^3 g^{-1}) are 23.9, 20.7, 21.0 and 18.2 kJ mol^{-1}, respectively. **ZJNU-61a**(Ho) exhibits higher C_2 hydrocarbon binding affinity than CH_4 throughout the adsorption process. The higher adsorption heats for C_2 hydrocarbons might be due to the comparable pore sizes in **ZJNU-61a**(Ho) with these small C_2 hydrocarbons. In addition, the open metal sites and heteroatoms within the framework may play a certain degree of contribution as it is well documented that these functional sites in MOFs are very beneficial for enhancing the binding energy between the framework and those easily polarized C_2 hydrocarbons gases.[15b] The higher heat of adsorption of C_2 hydrocarbons is thus responsible for the preferential adsorption of C_2 hydrocarbons over methane.

3.5 Thermal stability

As evidenced by the above TGA analysis, **ZJNU-61**(Ho) possesses a high decomposition temperature of 733 K under N_2 atmosphere. To further evaluate the thermal stability of **ZJNU-61**(Ho), we performed variable-temperature PXRD studies. Due to the limitation of equipment, the PXRD patterns were recorded only up to 623 K. As shown in Fig. 7a, the compound remains its integrity in the investigated temperature ranges. Since a small degradation of the framework will not be visible in the PXRD patterns as pointed out by Shimizu *et al.*,[16] we further assess the thermal stability by gas adsorption studies. The activated **ZJNU-61a**(Ho) was heated from room temperature to a specified temperature with a heating rate of 2 K min^{-1} under dynamic vacuum and maintained at that temperature for 30 min, and the porosity was then checked by nitrogen adsorption analyses at 77 K. It was found that the maximum amount of nitrogen adsorbed is similar to that of the sample activated at lower temperature until the activated temperature is increased to 523 K (Fig. 7b), indicating that the solvent-free framework can be thermally stable at least up to 473 K, which is really remarkable considering that the organic ligand is flexible. Such a good thermal stability might be attributed to the high connectivity of infinite "Ho-carboxylate" inorganic chain.

4 Conclusion

In summary, we have successfully constructed an Ln-MOF from a flexible cyclotriphosphazene-functionalized hexacarboxylate. The structure was characterized to be a 3D Ln-O rod-packing structure with 1D channels occupied by guest molecules. The rod-shaped SBU can not only prevent the formation of interpenetrating net but also significantly improve the thermal stability of the final framework. More importantly, despite the fact that the flexible organic ligand was used, the resulting LnMOF material after desolvation retained intact and exhibited selective adsorption of C_2 hydrocarbons over CH_4. Although the separation performance is not very impressive, this is a rare example of LnMOFs constructed from a flexible organic ligand exhibiting selective gas adsorption. Further exploration of more porous LnMOFs from other cyclotriphosphazene-functionalized multicarboxylate for their diverse applications is ongoing.

Acknowledgements

This work was supported by the Natural Science Foundation of China (No. 21301156), and the Natural Science Foundation of Zhejiang province, China (LR16B010001). The authors are thankful to the crystallographic reviewer for valuable comments and suggestions.

Reference

1 (a) Y. He, W. Zhou, G. Qian and B. Chen, *Chem. Soc. Rev.*, 2014, **43**, 5657-5678; (b) Y. He, B. Li, M. O'Keeffe and B. Chen, *Chem. Soc. Rev.*, 2014, **43**, 5618-5656; (c) J.-R. Li, J. Sculley and H.-C. Zhou, *Chem. Rev.*, 2012, **112**, 869-932; (d) K. Sumida, D. L. Rogow, J. A. Mason, T. M. McDonald, E. D. Bloch, Z. R. Herm, T.-H. Bae and J. R. Long, *Chem. Rev.*, 2012, **112**, 724-781; (e) H. Wu, Q. Gong, D. H. Olson and J. Li, *Chem. Rev.*, 2012, **112**, 836-868; (f) M. P. Suh, H. J. Park, T. K. Prasad and D.-W. Lim, *Chem. Rev.*, 2012, **112**, 782-835; (g) Y. He, W. Zhou, R. Krishna and B. Chen, *Chem. Commun.*, 2012, **48**, 11813-11831.

2 (a) M. Yoon, R. Srirambalaji and K. Kim, *Chem. Rev.*, 2012, **112**, 1196-1231; (b) A. Corma, H. García and F. X. L. i. Xamena, *Chem. Rev.*, 2010, **110**, 4606-4655; (c) J. Lee, O. K. Farha, J. Roberts, K. A. Scheidt, S. T. Nguyen and J. T. Hupp, *Chem. Soc. Rev.*, 2009, **38**, 1450-1459; (d) L. Ma, C. Abney and W. Lin, *Chem. Soc. Rev.*, 2009, **38**, 1248-1256.
3 L. E. Kreno, K. Leong, O. K. Farha, M. Allendorf, R. P. V. Duyne and J. T. Hupp, *Chem. Rev.*, 2012, **112**, 1105-1125.
4 P. Horcajada, R. Gref, T. Baati, P. K. Allan, G. Maurin, P. Couvreur, G. Férey, R. E. Morris and C. Serre, *Chem. Rev.*, 2012, **112**, 1232-1268.
5 P. Falcaro and S. Furukawa, *Angew. Chem. Int. Ed.*, 2012, **51**, 8431-8433.
6 B. Li, H.-M. Wen, Y. Cui, G. Qian and B. Chen, *Prog. Polym. Sci.*, 2015, **48**, 40-84.
7 (a) S. Pal, A. Bhunia, P. P. Jana, S. Dey, J. Mçllmer, C. Janiak and H. P. Nayek, *Chem. Eur. J.*, 2015, **21**, 2789-2792; (b) Q. Yao, A. B. Gómez, J. Su, V. Pascanu, Y. Yun, H. Zheng, H. Chen, L. Liu, H. N. Abdelhamid, B. n. Martín-Matute and X. Zou, *Chem. Mater.*, 2015, **27**, 5332-5339; (c) B. Liu, W.-P. Wu, L. Hou and Y.-Y. Wang, *Chem. Commun.*, 2014, **50**, 8731-8734; (d) W. Mu, X. Huang, R. Zhong, W. Xia, J. Liu and R. Zou, *CrystEngComm*, 2015, **17**, 1637-1645; (e) H. Li, W. Shi, K. Zhao, Z. Niu, H. Li and P. Cheng, *Chem. Eur. J.*, 2013, **19**, 3358-3365; (f) K. Tang, R. Yun, Z. Lu, L. Du, M. Zhang, Q. Wang and H. Liu, *Cryst. Growth Des.*, 2013, **13**, 1382-1385; (g) Y.-P. He, Y.-X. Tan and J. Zhang, *Inorg. Chem.*, 2013, **52**, 12758-12762; (h) Y. He, H. Furukawa, C. Wu, M. O'Keeffe and B. Chen, *CrystEngComm*, 2013, **15**, 9328-9331; (i) Y. He, H. Furukawa, C. Wu, M. O'Keeffe, R. Krishna and B. Chen, *Chem. Commun.*, 2013, **49**, 6773-6775; (j) Z. Lin, R. Zou, W. Xia, L. Chen, X. Wang, F. Liao, Y. Wang, J. Lin and A. K. Burrell, *J. Mater. Chem.*, 2012, **22**, 21076-21084; (k) Y. He, S. Xiang, Z. Zhang, S. Xiong, F. R. Fronczek, R. Krishna, M. O'Keeffee and B. Chen, *Chem. Commun.*, 2012, **48**, 10856-10858; (l) Z. Guo, H. Xu, S. Su, J. Cai, S. Dang, S. Xiang, G. Qian, H. Zhang, M. O'Keeffe and B. Chen, *Chem. Commun.*, 2011, **47**, 5551-5553; (m) H.-L. Jiang, N. Tsumori and Q. Xu, *Inorg. Chem.*, 2010, **49**, 10001-10006; (n) S. Ma, X.-S. Wang, D. Yuan and H.-C. Zhou, *Angew. Chem. Int. Ed.*, 2008, **47**, 4130-4133; (o) Y. K. Park, S. B. Choi, H. Kim, K. Kim, B.-H. Won, K. Choi, J.-S. Choi, W.-S. Ahn, N. Won, S. Kim, D. H. Jung, S.-H. Choi, G.-H. Kim, S.-S. Cha, Y. H. Jhon, J. K. Yang and J. Kim, *Angew. Chem. Int. Ed.*, 2007, **46**, 8230-8233; (p) X. Guo, G. Zhu, Z. Li, F. Sun, Z. Yang and S. Qiu, *Chem. Commun.*, 2006, 3172-3174; (q) T. Devic, C. Serre, N. Audebrand, J. Marrot and G. Férey, *J. Am. Chem. Soc.*, 2005, **127**, 12788-12789; (r) T. M. Reineke, M. Eddaoudi, M. Fehr, D. Kelley and O. M. Yaghi, *J. Am. Chem. Soc.*, 1999, **121**, 1651-1657.
8 Y. Ling, C. Song, Y. Feng, M. Zhang and Y. He, *CrystEngComm*, 2015, **17**, 6314-6319.
9 (a) S.-Z. Liu, X. Wu, A.-Q. Zhang, J.-J. Qiu and C.-M. Liu, *Langmuir*, 2011, **27**, 3982-3990; (b) H. A. Alidağı, Ö. M. Gırgıç, Y. Zorlu, F. Hacıvelioğlu, S. Ü. Çelik, A. Bozkurt, A. Kılıç and S. Yeşilot, *Polymer*, 2013, **54**, 2250-2256; (c) P. Mohanty, L. D. Kull and K. Landskron, *Nat. Commun.*, 2011, **2**, 401.
10 (a) B. Li, X. Dai, X. Meng, T. Zhang, C. Liu and K. Yu, *Dalton Trans.*, 2013, **42**, 2588-2593; (b) B. Li, X. Chen, F. Yu, W. Yu, T. Zhang and D. Sun, *Cryst. Growth Des.*, 2014, **14**, 410-413.
11 (a) A. L. Spek, Acta Cryst., 2009, D65, 148–155; (b) A. L. Spek, Acta Cryst., 2015, C71, 9–18.
12 H. Zhang, N. Li, C. Tian, T. Liu, F. Du, P. Lin, Z. Li and S. Du, *Cryst. Growth Des.*, 2012, **12**, 670-678.
13 (a) B. Liu, S. Yao, C. Shi, G. Li, Q. Huo and Y. Liu, *Chem. Commun.*, 2016, **52**, 3223-3226; (b) Y.-X. Tan, Y.-P. He and J. Zhang, *RSC Adv.*, 2015, **5**, 7794-7797; (c) J. Li, H.-R. Fu, J. Zhang, L.-S. Zheng and J. Tao, *Inorg. Chem.*, 2015, **54**, 3093-3095; (d) Q.-G. Zhai, N. Bai, S. n. Li, X. Bu and P. Feng, *Inorg. Chem.*, 2015, **54**, 9862-9868; (e) K. Liu, D. Ma, B. Li, Y. Li, K. Yao, Z. Zhang, Y. Han and Z. Shi, *J. Mater. Chem. A*, 2014, **2**, 15823-15828; (f) J. Jia, L. Wang, F. Sun, X. Jing, Z. Bian, L. Gao, R. Krishna and G. Zhu, *Chem. Eur. J.*, 2014, **20**, 9073-9080; (g) J. Duan, M. Higuchi, S. Horike, M. L. Foo, K. P. Rao, Y. Inubushi, T. Fukushima and S. Kitagawa, *Adv. Funct. Mater.*, 2013, 3525-3530; (h) N. Nijem, H. Wu, P. Canepa, A. Marti, J. Kenneth J. Balkus, T. Thonhauser, J. Li and Y. J. Chabal, *J. Am. Chem. Soc.*, 2012, **134**, 15201-15204; (i) Y. He, Z. Zhang, S. Xiang, F. R. Fronczek, R. Krishna and B. Chen, *Chem. Commun.*, 2012, **48**, 6493-6495; (j) Y. He, Z. Zhang, S. Xiang, H. Wu, F. R. Fronczek, W. Zhou, R. Krishna, M. O'Keeffe and B. Chen, *Chem. Eur. J.*, 2012, **18**, 1901-1904; (k) Y. He, Z. Zhang, S. Xiang, F. R. Fronczek, R. Krishna and B. Chen, *Chem. Eur. J.*, 2012, **18**, 613-619; (l) J. v. d. Bergh, C. Gücüyener, E. A. Pidko, E. J. M. Hensen, J. Gascon and F. Kapteijn, *Chem. Eur. J.*, 2011, **17**, 8832-8840.
14 H. Xu, J. Cai, S. Xiang, Z. Zhang, C. Wu, X. Rao, Y. Cui, Y. Yang, R. Krishna, B. Chen and G. Qian, *J. Mater. Chem. A*, 2013, **1**, 9916-9921.
15 (a) Y. He, R. Krishna and B. Chen, *Energy Environ. Sci.*, 2012, **5**, 9107-9120 ; (b) E. D. Bloch, W. L. Queen, R. Krishna, J. M. Zadrozny, C. M. Brown and J. R. Long, *Science*, 2012, **335**, 1606-1610.
16 B. S. Gelfand and G. K. H. Shimizu, *Dalton Trans.*, 2016, **45**, 3668-3678.
17

TOC

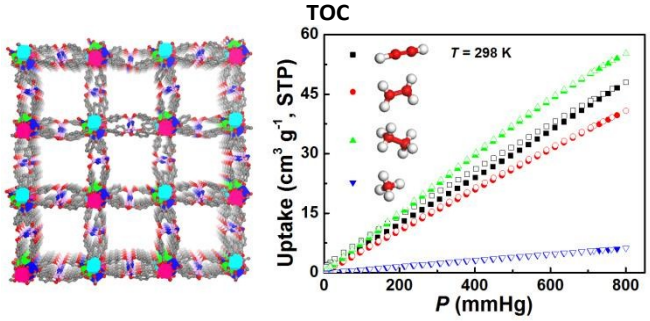

This work presents a rare example of permanently porous lanthanide based metal-organic frameworks based on flexible cyclotriphosphazene-functionalized hexacarboxylate exhibiting the potential for selective adsorption of C_2 hydrocarbons over methane at ambient temperature.